Int. J. Heat Mass Transfer. Vol. 29, No. 6, pp. 927–939, 1986
Printed in Great Britain

0017–9310/86 $3.00 + 0.00
Pergamon Journals Ltd.

Annular film-flow boiling of liquids in a partially heated, vertical channel with offset strip fins

V. P. CAREY and G. D. MANDRUSIAK
Department of Mechanical Engineering, University of California, Berkeley, CA 94720 U.S.A.

(*Received* 4 *September* 1985 *and in final form* 31 *December* 1985)

Abstract—Flow visualization photographs and measured local heat transfer data are presented for annular film-flow boiling of saturated liquids in a vertical channel with offset strip fins. A special test section was used in this study which permitted direct visual observation of the boiling process while simultaneously measuring local heat transfer coefficients at several locations along the channel. One wall of the channel was heated while the opposite and lateral walls were adiabatic. Measured local heat transfer coefficients on the heated portion of the channel wall were obtained for convective boiling of water, methanol and *n*-butanol at atmospheric pressure over wide ranges of mass flux and quality. Photographs of the flow indicate that virtually no nucleate boiling is present when the flow is in the film-flow regime. For the fin matrix studied here, complete dryout of the film on the heated surface was not observed to occur at a single downstream location. Instead, dry patches are observed to form at specific locations in the matrix, with the patches increasing in size with downstream distance until the entire film is gone. An approximate analytical model of transport in the liquid film is also presented. A closed-form correlation for the boiling heat transfer coefficient is derived from this model which is in good agreement with our measured data.

INTRODUCTION

IT HAS been common practice for many years to use offset strip fin geometries in compact heat exchangers for single-phase heat transfer applications. However, in recent years, efforts to achieve weight savings or improve efficiency have resulted in the increasing use of offset strip fin surfaces for evaporators and condensers in refrigeration, air-conditioning and cryogenic systems. Boiling of a liquid coolant in a geometry of this type may also prove to be an effective means of cooling electronic components or fusion reactor walls under high heat flux conditions. Larger-scale offset fin geometries may also provide high-efficiency condenser or evaporator surfaces in desalination systems.

Interest in the applications noted above has prompted several recent studies of convective boiling in offset strip fin geometries. Panitsidis *et al.* [1] measured the total heat transfer for a heat exchanger with offset strip fins operating as a thermosyphon boiler with R-113 and isopropanol. They also developed a multi-node analysis for boiling over one fin to model the transport. This model neglected the effect of fluid velocity on heat transfer and assumed that the boiling heat transfer coefficient depended only on the local wall superheat. In a later study, Chen *et al.* [2] refined this technique to include the velocity effect. Values of the total heat duty predicted by this technique were found to be in good agreement with corresponding measured results at moderate to high wall superheat [2, 3].

Galezha *et al.* [4] also obtained measurements of heat transfer coefficients for thermosyphon boiling of R-12 and R-22 in several strip fin geometries. They provided correlations for their test data, based on thermodynamic similitude, which accounted for the effects of heat flux, pressure and fluid properties on heat transfer.

The studies described above all consider moderate to high wall superheat levels where nucleate boiling effects are expected to play an important role. In a series of recent papers, Robertson [5–7] and Robertson and Lovegrove [8] have investigated flow boiling processes in a channel with offset strip fins at very low wall superheat levels. For the conditions considered in these studies, nucleate boiling effects were negligible and forced convective boiling was the dominant mode of vaporization. Measured local heat transfer coefficients were presented for nitrogen [5] and R-11 [8] for wide ranges of mass flow rate and local quality. Film-flow models [6, 7] were also proposed to predict boiling heat transfer coefficients for offset strip fins.

In a recent study, Yung *et al.* [9] also proposed a film-flow model for forced convective boiling and condensation in offset fin geometries. The predictions of this model were found to agree well with available data for forced convective boiling in offset fin geometries.

The studies described above have provided valuable insight into the nature of convective boiling in offset fin geometries. However, despite these efforts, there are several aspects of the transport for these conditions that have not been thoroughly explored. Although film-flow models have been proposed in several previous studies, none of them have attempted to visually observe and verify the two-phase flow regime. Even if flow regime predictions for vertical round tubes are used, the results may be inconclusive. For example, most of the data of Robertson [5] for convective boiling of liquid nitrogen appear to be very close to the

NOMENCLATURE

A constant in equation (13)
A_f surface area of fins in channel section of length L_c
A_P prime surface area of channel section of length L_c
A_o cross-sectional open area of channel
c_p specific heat at constant pressure
d_h hydraulic diameter based on wetted perimeter, $4A_o/P_W$
d_{hp} hydraulic diameter based on heated perimeter, $4A_o/P_H$
f friction factor
G mass flux
h heat transfer coefficient
H dimension of fins from root to tip
j_f volume flux of liquid, $G(1-x)/\rho_f$
j_g volume flux of vapor, Gx/ρ_g
j_g^* dimensionless volume flux of vapor, $j_g\rho_g^{1/2}[gd_h(\rho_f-\rho_g)]^{-1/2}$
k fluid thermal conductivity
k_c conductivity of copper
L length of fin in the downstream direction
L_c length of channel section
n exponent in equation (13)
p pressure
P_H heated perimeter
P_W wetted perimeter
Pr_f liquid Prandtl number
Pr_t turbulent Prandtl number in liquid film
q'' surface heat flux
Re_f liquid Reynolds number, $G(1-x)d_h/\mu_f$
Re_g vapor Reynolds number, Gxd_h/μ_g
Re_{fp} liquid Reynolds number based on heated perimeter, $G(1-x)d_{hp}/\mu_f$
St Stanton number, h/Gc_p
t fin thickness
T_W wall temperature of prime surface of channel
T_M bulk mean temperature of the coolant
T_{SAT} saturation temperature of coolant
u downstream local velocity in liquid film
u^+ dimensionless u velocity, $u/\sqrt{\tau_o/\rho_f}$
W_c width of copper slab
x mass quality
y coordinate normal to the channel wall
y^+ dimensionless y coordinate, $y\sqrt{\tau_o/\rho_f}/\nu_f$
X_{tt} Martinelli parameter for turbulent–turbulent flow, $[(dp/dz)_{Ff}/(dp/dz)_{Fg}]^{1/2}$.

Greek symbols
δ^+ value of y^+ at the liquid–vapor interface
ε_M turbulent eddy diffusivity of momentum
κ Von Karman constant
μ absolute viscosity
ν kinematic viscosity
ϕ_f two-phase multiplier, $[(dp/dz)_{Ftp}/(dp/dz)_{Ff}]^{1/2}$
Ψ parameter defined in equation (24)
τ_o shear stress at the channel wall.

Subscripts
f liquid properties or corresponding to liquid flow alone in the channel
g vapor properties or corresponding to vapor flow alone in the channel
fp corresponding to liquid flow alone in the channel heated on one side only
F friction component of pressure gradient
tp corresponding to two-phase flow conditions.

transition between churn flow and annular flow. On the flow regime map of Hewitt and Roberts [10], some of these data would be in the annular flow regime, and some would be in the churn flow regime. Yet the steady turbulent film flow models do a reasonably good job of predicting the heat transfer for all these data. More information regarding the two-phase flow behavior during convective boiling in offset fin geometries is needed to guide the development and evaluation of analytical models of the transport. In addition, heat transfer data have been obtained only for a few specific geometries and fluids. More data is needed to fully assess the effects of geometry variations on transport.

The present study was undertaken to achieve three main objectives. The first objective was to obtain heat transfer measurements for a channel with offset strip fins with the channel heated on one side only. Although heating of a coolant channel on one side may arise in electronics cooling and other applications, the previous studies mentioned above have only considered channels heated on both sides. Although this study specifically sought to examine the heat transfer characteristics for one-sided heating, the results also provide insight into the boiling mechanisms which occur when both sides are heated.

The second objective of this study was to gain a better understanding of the relation between the two-phase flow behavior and convective boiling heat transfer in offset fin geometries. We specifically wanted to determine the flow regime associated with various combinations of quality and mass flux through the channel. We also wanted to identify any nonsymmetric behavior associated with the one-sided heating.

The third objective was to examine the variation of the convective boiling heat transfer performance with liquid Prandtl number as the Prandtl number

increases. To achieve these objectives, experiments were conducted using a special test section which permitted us to observe visually the two-phase flow during convective boiling in a channel with offset strip fins. This test section also permitted simultaneous measurement of local values of the convective boiling heat transfer coefficient in the channel.

This study specifically focused on the behavior of vertical flows at moderate to high quality levels where the two-phase flow is almost always in an annular film-flow configuration. Measured values of the local heat transfer coefficient are presented for saturated flow boiling of water, methanol and *n*-butanol at atmospheric pressure. At saturation, the Prandtl numbers of the liquids tested here cover the range of moderate values from 1.8 to 8.6. Using an approximate analysis of transport in the liquid film, a correlation for the local convective boiling heat transfer coefficient is also derived and compared with our experimental data. The observed two-phase flow behavior and dryout characteristics are also discussed.

EXPERIMENTAL APPARATUS

To study the convective boiling process in offset fin geometries, the special test section shown in Fig. 1 was constructed. One end of the rectangular copper slab shown in Fig. 1 was machined to form a surface with offset strip fins. This end of the copper slab fits into the assembly in Fig. 1 to form a channel with offset strip fins. The side walls of the channel are Teflon to minimize lateral heat loss, and the inner glass plate forms the top wall of the channel to permit visual observation of the boiling process all along the channel.

A thin coating of RTV silicone sealant was applied to the top edges of the fins to eliminate heat leakage to the glass cover plate. A second glass plate covers the inner one as shown in Fig. 1 to reduce heat losses from the top of the assembly. The channel formed by the Teflon side walls, inner glass plate and copper slab is 1.91 cm wide, 3.8 mm high and 45.7 cm long. The fins machined in the copper slab are 1.59 mm thick, 12.7 mm long in the flow direction, and extend to the top (glass) wall of the channel (3.8 mm high). The distance between adjacent fins is 7.94 mm. The hydraulic diameter based on the heated perimeter for this surface, d_{hp}, is 7.78 mm. Note that the hydraulic diameter based on wetted perimeter, d_h, is smaller ($d_h = 5.15$ mm).

The copper slab was heated at the bottom end by two electrical resistance heaters. These heaters provided a virtually uniform heat input along the length of the channel. Heat is conducted from the heaters along the copper slab to the finned surface where it is transferred to the fluid in the channel. The back of the copper slab and heater assembly was completely enclosed in insulation so that heat leakage to the surroundings was negligible.

Thermocouples were embedded in the copper slab, as indicated in Fig. 1, to determine the temperature gradient and surface temperature at three locations along the length of the channel. Thermocouples were also installed through the channel wall at these same locations to measure the local fluid temperature. The measured temperature gradient was used to calculate the heat flux to the surface. This result was combined with the measured local fluid and surface temperatures to compute the local heat transfer coefficient.

The system shown in Fig. 2 was used to provide a steady flow of liquid to the test section. The power to the auxiliary heaters in the reservoir and the condenser

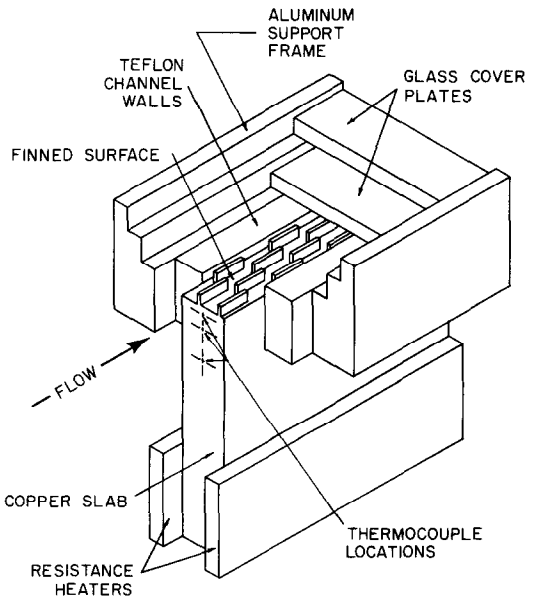

FIG. 1. Cutaway view of test section (not to scale).

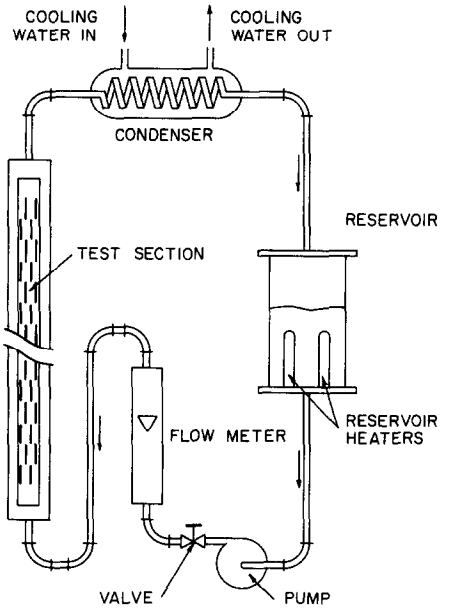

FIG. 2. Test system used in convective boiling experiments.

water flow rate could be varied to control the level of subcooling of the liquid at the inlet to the test section. The flow rate to the test section was controlled by the flow control valve and also by varying the power input to the pump.

The liquid flow rate to the test section was measured using a Cole–Parmer rotameter. This flow meter was calibrated by measuring the flow output of the system over a specified interval of time at different float positions. Such measurements were done at several liquid temperatures so that the effect of property variation with temperature was taken into account. Rotameter calibration curves were thereby determined for each of the fluids tested here: water, methanol and *n*-butanol.

Prior to running the heat transfer experiments, the finned surface of the copper slab was cleaned with a mild acid solution and then thoroughly rinsed before filling the system with the test liquid. This procedure kept the finned copper surface clean and free of tarnish throughout the test program.

Although Fig. 1 depicts the test section channel horizontally, all experiments reported here were done with the channel in a vertical position with the flow upward. Power to the heaters in the test section was provided by two rheostats, which could be adjusted to control the heat input to the channel. Copper–constantan thermocouples in the test section were read using an Omega two-pole selector switch and a precision Fluke digital readout. Photographs of the two-phase flow at various locations along the channel were taken using a Pentax 35-mm camera with a 50-mm macro lens and an automatic strobe flash unit. The strobe unit provides flash pulses as short as 0.0001 s to freeze the very rapid motion of the two-phase flow.

EXPERIMENTAL PROCEDURE AND RESULTS

Before running the convective boiling experiments, the single-phase heat transfer characteristics were determined for the channel with offset strip fins in the test section. Local heat transfer coefficients were measured at low heat flux and high inlet subcooling where no vaporization occurs. After setting the flow rate and power to the heaters at the desired levels, the system was allowed to stabilize for 10–15 min before thermocouple and flow readings were taken. The resulting single-phase heat transfer data for water are plotted in non-dimensional form in Fig. 3. The heat transfer coefficients represented in Fig. 3 were measured at a specific downstream location and they are average values over the heated perimeter of the channel at that location. These values of h were iteratively calculated from the energy balance relation:

$$W_c I_c k_c \nabla T_c = h(A_P + \eta_F A_F)(T_W - T_M) \qquad (1)$$

where ∇T_c is the measured local temperature gradient

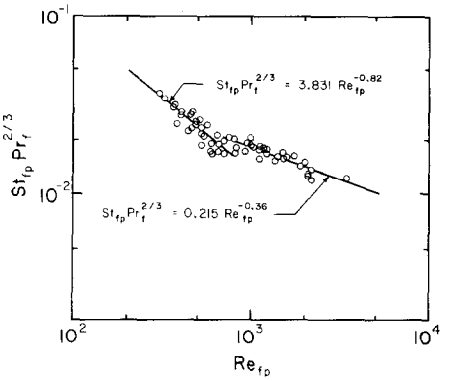

FIG. 3. Single-phase heat transfer data for test section channel.

in the copper and η_F is the fin efficiency given by

$$\eta_F = \frac{\tanh(MH)}{MH}, \quad M = \sqrt{2h(t+L)/k_c tL}. \qquad (2)$$

The trend in the data in Fig. 3 suggests that the transition to turbulent flow occurs at a Reynolds number of about 750. The correlations shown in Fig. 3 for the laminar and turbulent ranges are least-squares fits to the data below $Re = 750$ and above $Re = 750$, respectively. The single-phase heat transfer correlation for turbulent flow will be discussed further in connection with boiling heat transfer data.

For the flow boiling experiments, the system was allowed to stabilize at the selected power and flow settings before flow visualization photographs or data were taken. The thermocouple readings and the liquid flow rates were recorded in the same manner as for the single-phase data. The downstream location where saturated nucleate boiling first began was also determined by visually inspecting the flow in the channel. This zero-quality point was taken to be the lowest vertical location where continuous growth and release of vapor bubbles occurred and vapor bubbles were present throughout the liquid flow in the channel.

The heat transfer coefficient was determined at the two uppermost thermocouple locations where boiling was observed to occur. As for single-phase flow, the local heat transfer coefficient was obtained by iteratively solving equations (1) and (2) using the measured data at the location of interest. The only difference was that in equation (1), T_M was equal to T_{SAT}, the saturation temperature of the coolant. The boiling heat transfer coefficients calculated in this manner are average values over the heated perimeter of the channel.

The mass flux, G, was determined from the flow meter reading and the geometry of the channel. The quality at the two uppermost thermocouple locations was determined by using the measured heat input values in an energy balance over the portion of the channel where saturated boiling occurred. The measurements thus indicated the value of h_{tp} which corresponded to specific values of x and G.

Values of h_{tp} were determined for convective boiling of water, methanol and *n*-butanol. Data have been obtained for values of quality and mass flux in the ranges $0.05 < x < 0.7$ and $3 < G < 100$ kg m^{-2} s^{-1}. The estimated uncertainty in the measurements is less than $\pm 5\%$ for G, $\pm 7\%$ for x and $\pm 11\%$ for h_{tp}.

The flow conditions at which data were obtained are indicated on a flow-regime map of the type proposed by Hewitt and Roberts [10] for upward co-current flow in Fig. 4. It can be seen that the flow conditions studied here are close to the transition from churn flow to annular flow. The transition line suggested by Hewitt and Roberts [10] corresponds approximately to $\rho_g j_g^2 = 200$ for the range of $\rho_f j_f^2$ encountered in our experiments. This would place all of our data in the churn flow regime. For the fluids considered here, the transition condition suggested by Wallis [11] is much lower, but it would also place much of our data in the churn flow region.

Our visual observations indicated that for virtually all our data, the flow in the channel was annular in configuration. However, for about 40% of the data points, the flow appeared slightly oscillatory in nature with visible intermittant downflow of liquid. For these conditions, which usually occurred at lower qualities, the flow looked more like churn flow than steady annular flow. The other 60% of the data appeared to be in upward annular flow.

The approximate transition line between churn and annular flow, based on our visual observations, is indicated in Fig. 4. The observed transition lines for the three fluids tested here were virtually identical on the type of plot shown in Fig. 4. In terms of the j_g^* parameter defined by Wallis [11], the transition conditions observed for the three fluids studied here correspond approximately to $j_g^* = 0.5$.

Photographs of the boiling process in the channel at different stages are shown in Figs. 5–8. Figure 5 shows

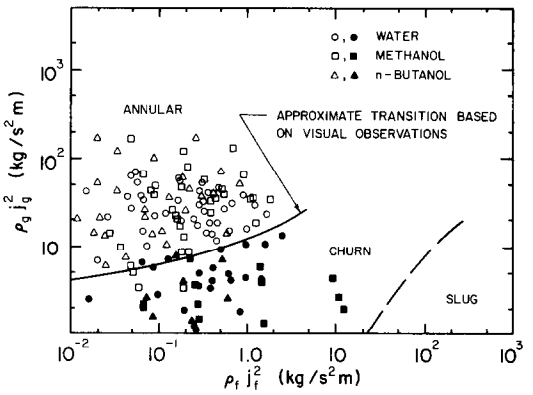

FIG. 4. Visually observed, two-phase flow regimes during convective boiling in a channel with offset strip fins. The solid symbols designate churn flow and the open symbols designate annular film flow. The broken line is the transition between slug and churn flow indicated on the flow regime map of Hewitt and Roberts [10] for vertical flow in tubes.

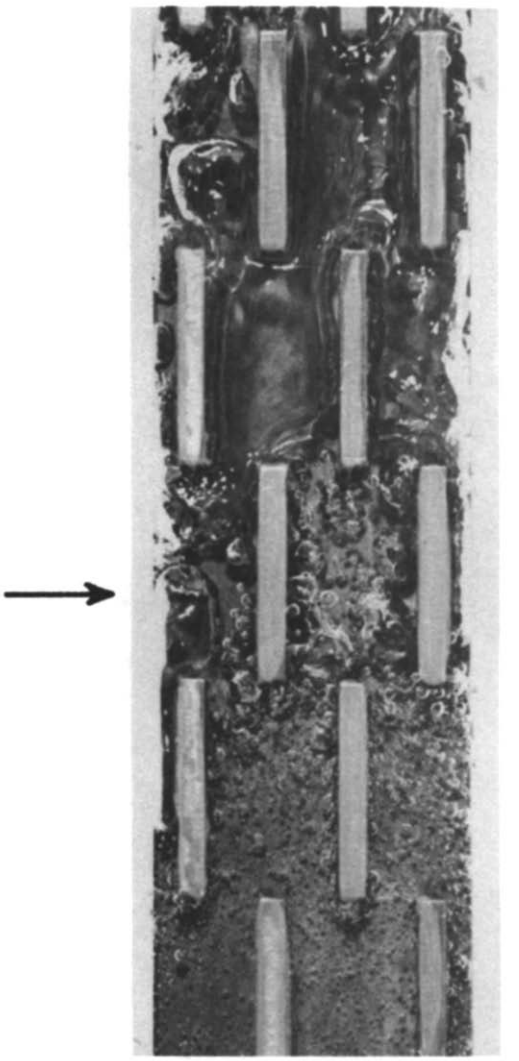

FIG. 5. Photograph of the onset of saturated boiling of water in a vertical channel with offset strip fins. The mass flux is 12.5 kg m^{-2} s^{-1}. At the thermocouple location indicated by the arrow, $q'' = 39.5$ kW m^{-2}, $x = 0.01$ and $h_{tp} = 6.73$ kW m^{-2} K^{-1}.

the onset of saturated boiling for water at a mass flux of 12.5 kg m^{-2} s^{-1}. At the thermocouple location indicated by the arrow in the figure, the heat flux was 39.5 kW m^{-2}, $T_W - T_{SAT}$ was 6.2°C and h_{tp} was 6.73 kW m^{-2} K^{-1}. At this location, which is just downstream of the point where saturated boiling begins, nucleate boiling appears to be the dominant heat transfer mechanism. It can also be seen in Fig. 5 that only a short distance downstream, the flow has undergone a transition to slug flow (recall that the fins are only 12.7 mm long). A short distance thereafter, the transition from slug flow to an annular configuration was observed. A rapid transition from bubbly flow to an annular flow configuration was characteristic of the boiling processes for all three fluids tested here.

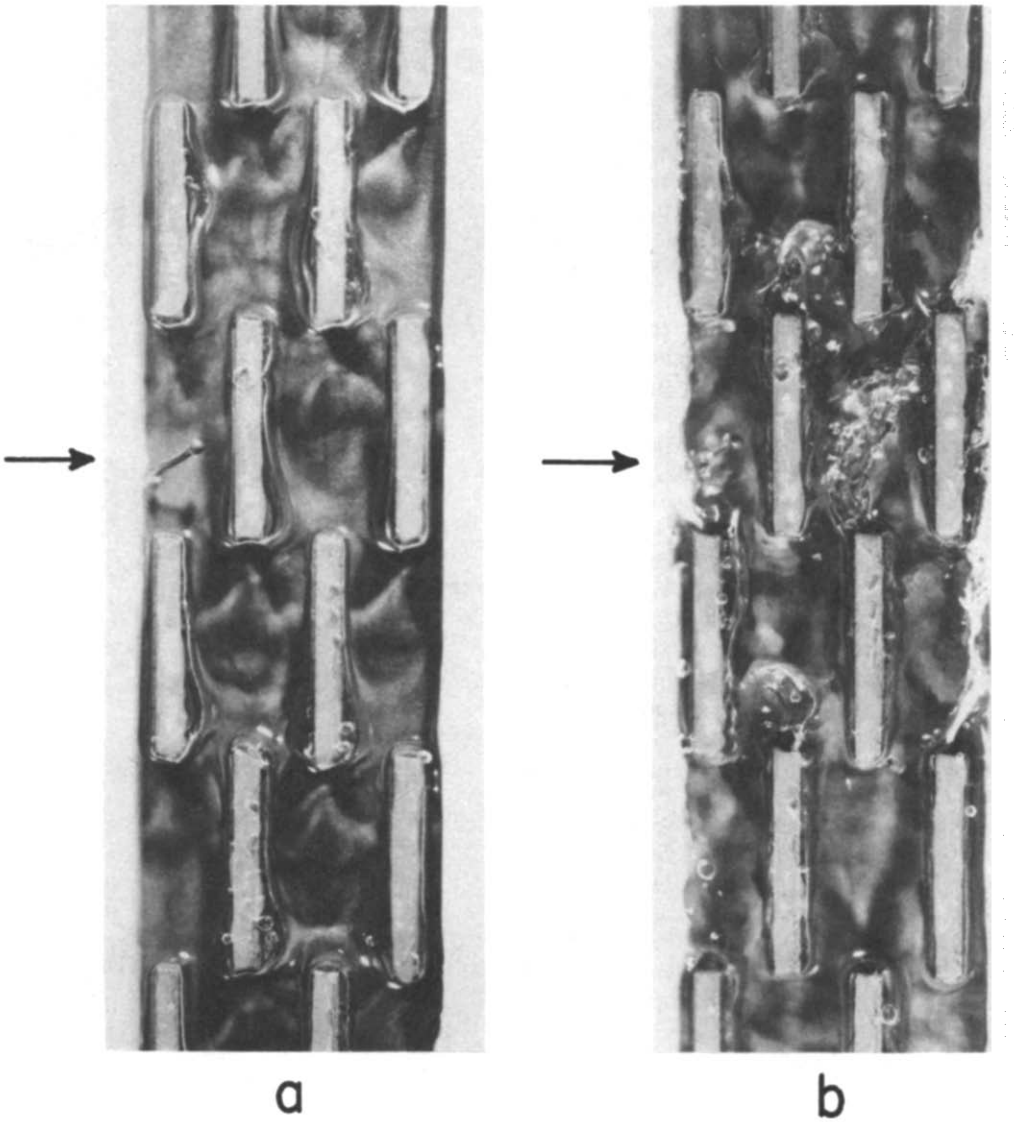

FIG. 6. Photographs of annular film-flow boiling of water in a vertical channel with offset strip fins. Both photographs were taken at the same location at different times for $G = 21.5\ \text{kg m}^{-2}\ \text{s}^{-1}$ and $q'' = 83.4\ \text{kW m}^{-2}$. At the thermocouple location indicated by the arrow, $x = 0.24$ and $h_{tp} = 20.6\ \text{kW m}^{-2}\ \text{K}^{-1}$.

Photographs of the annular, two-phase flow observed during the convective boiling of water and methanol are shown in Figs. 6 and 7, respectively. Figure 6 shows two photographs taken at the same conditions and downstream location at different times. At the thermocouple location indicated by the arrow, $G = 21.5\ \text{kg m}^{-2}\ \text{s}^{-1}$, $x = 0.24$ and $h_{tp} = 20.6\ \text{kW m}^{-2}\ \text{K}^{-1}$. Most of the time the flow looked like that shown in Fig. 6a. Visually it appeared that the film traveling along the front and the back surfaces piles-up at the upstream ends of the fins. Intermittantly, waves could be observed to travel upward in the liquid film along the front and back walls of the channel. When this occurred, some of the liquid which had accumulated at the upstream end of the fin was shed off the downstream end. A photograph capturing this shedding process is shown in Fig. 6b.

The annular flow behavior observed during convective boiling of methanol and *n*-butanol was very similar to that observed for water. Two photographs of the annular two-phase flow in the channel during convective boiling of methanol are shown in Fig. 7. The flow conditions are indicated in the figure caption. Figure 7a shows relatively undisturbed upward annular flow, whereas Fig. 7b shows the intermittent shedding of liquid off the downstream end of the fin. The shedding mechanism appeared to the same as for water. It can be seen in Figs. 6b and 7b that for the geometry

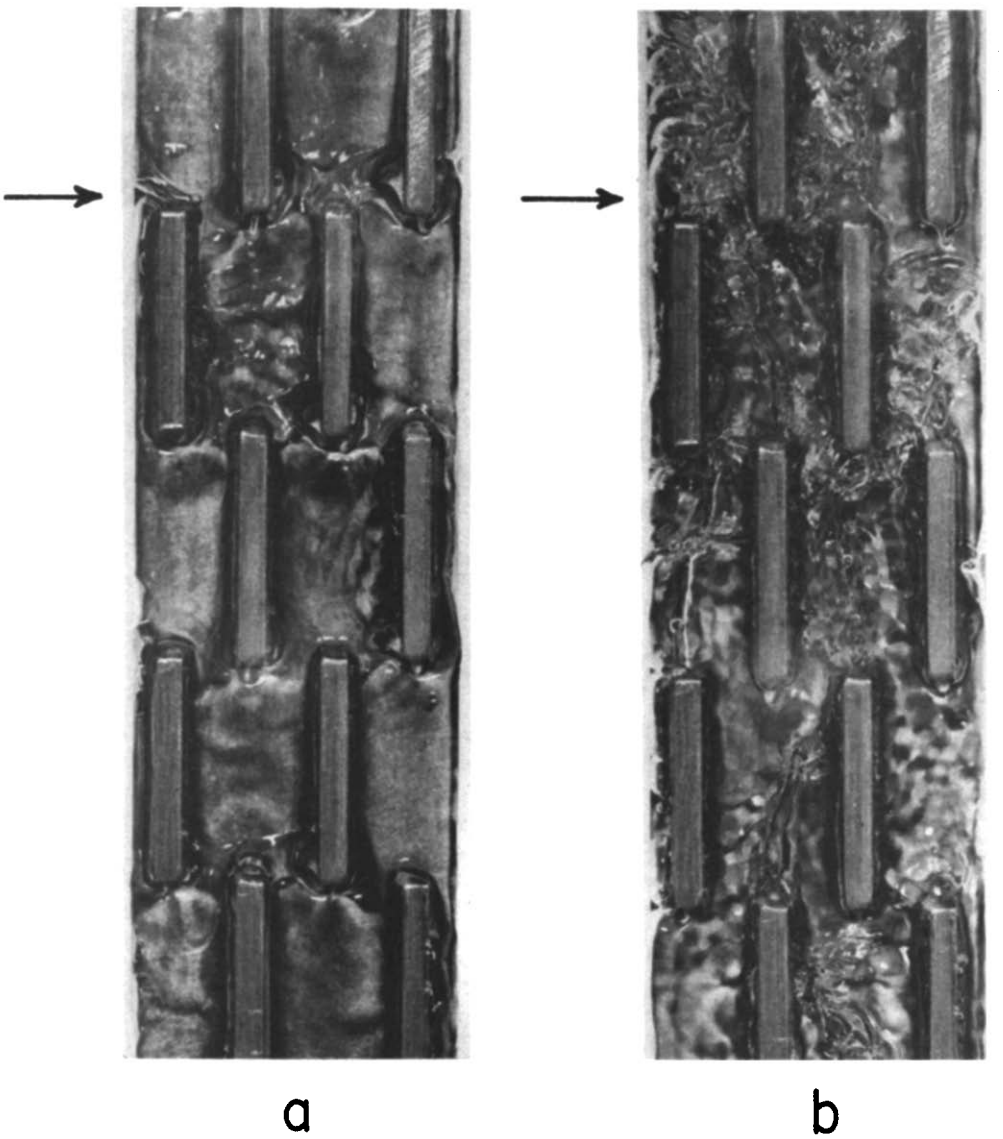

FIG. 7. Photographs of annular film-flow boiling of methanol in a vertical channel with offset strip fins. Both photographs were taken at the same location at different times for $G = 15.0$ kg m^{-2} s^{-1} and $q'' = 23.9$ kW m^{-2}. At the thermocouple location indicated by the arrow, $x = 0.22$ and $h_{tp} = 4.47$ kW m^{-2} K^{-1}.

studied here, this shed liquid appears to interact almost immediately with the liquid films along the front and back walls of the channel.

This intermittent shedding of liquid from the fins was most often observed at the lower quality end of the annular flow region of the channel, where more liquid is present. Visually, this process appeared to cause only a minor fluctuation in the flow, and no fluctuations in the flow rate or thermocouple readings were detected when it was observed. Even when churn flow was observed over a portion of the channel, no significant fluctuations in the flow or temperature readings were observed.

It can be seen in Figs. 6 and 7 that there is virtually no nucleate boiling present, even though the superheat of the prime surface is over 4°C. In a few locations, bubbles can be observed in the corner where the fin meets the glass or copper surface. The convective component of heat transport is expected to be weaker, and the liquid film is thicker in these corner regions. Consequently, there will be less tendency to suppress nucleation there. Hence, it is not surprising that nucleation persists at a few points at these locations, even though it has been thoroughly suppressed along the flat surfaces of the channel.

Figure 8 shows a photograph of the two-phase flow near the upper end of the channel, where dry patches on the heated surface were first observed. This photo-

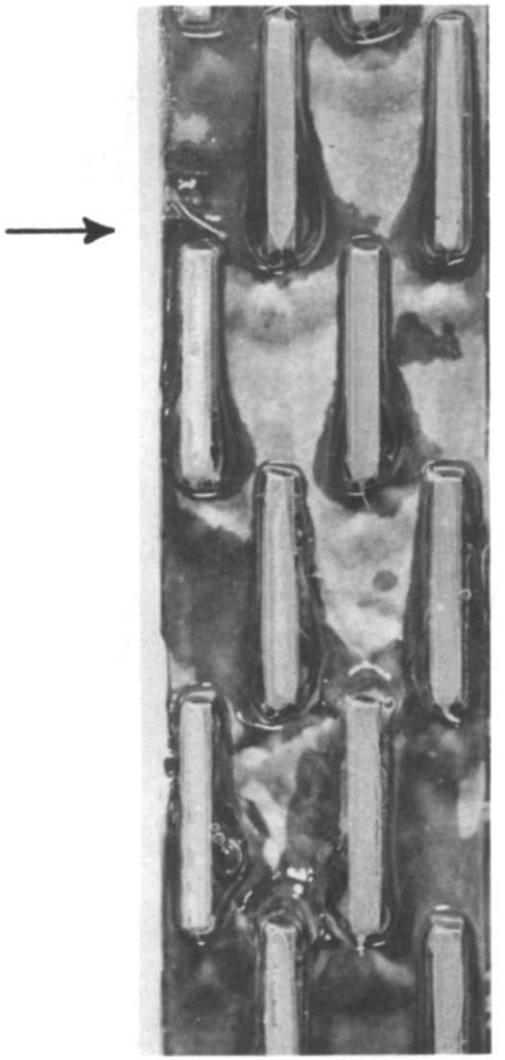

FIG. 8. Photograph of annular film flow boiling of water in a channel with offset strip fins at $G = 12.5$ kg m^{-2} s^{-1} and $q'' = 77.3$ kW m^{-2} s^{-1}. The light regions on the surface are dry areas and the darker regions are covered with liquid. At the thermocouple location indicated by the arrow, $x = 0.38$ and $h_{tp} = 15.1$ kW m^{-2} K^{-1}.

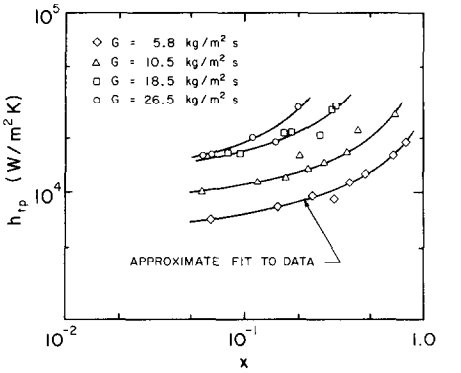

FIG. 9. Measured local heat transfer coefficients for convective boiling of water in a vertical channel with offset strip fins.

graph was taken during convective boiling of water. At the thermocouple location indicated by the arrow, $G = 12.5$ kg m^{-2} s^{-1}, $x = 0.38$ and $h_{tp} = 15.1$ kW m^{-2} K^{-1}. The light patches on the back wall of the channel are dry areas, whereas darker portions of the surface are still covered with the liquid film. At the lower edge of this photograph, the walls are almost completely covered with liquid. As one proceeds downstream, the size of the dryout patches increases. For tests at high heat flux and low mass flux, the dry patches increased in size with downstream distance until the entire channel was dry.

The dryout characteristics of the channel tested here are affected in a strong way by the geometry. It should be noted that in annular flow, a liquid film is traveling upward along the adiabatic front wall of the channel. When it encounters the upstream end of a fin, liquid from the film on the adiabatic wall may be transferred by vapor shear and surface tension forces onto the fin, and subsequently onto the prime surface. This transfer of liquid tends to keep the fins and the prime surface near the upstream end of the fin wet, even when much of the prime surface is dry. Hence, in channels heated on one side only, offset strip fins may facilitate transfer of liquid from the unheated wall to the heated wall and thereby prevent the heated surface from drying out completely at high qualities.

It can also be seen in Fig. 8 that at a few locations nucleate boiling appears to occur. As in Figs. 6 and 7, bubbles are visible only in the corner locations where the liquid film tends to be thicker, and there is less of a tendency to suppress nucleate boiling. When dry patches existed on the channel walls during the experiments, in general, the size and shape of the dryout patches were observed to change with time. In particular, waves in the liquid film were sometimes observed to carry liquid downstream which would momentarily reduce the size of the dry patches.

The experimentally determined variations of h_{tp} with x for various G values are shown in Figs. 9, 10 and 11 for

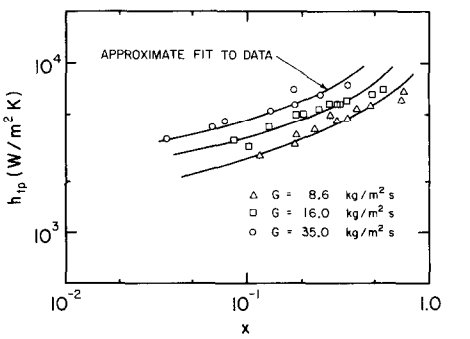

FIG. 10. Measured local heat transfer coefficients for convective boiling of methanol in a vertical channel with offset strip fins.

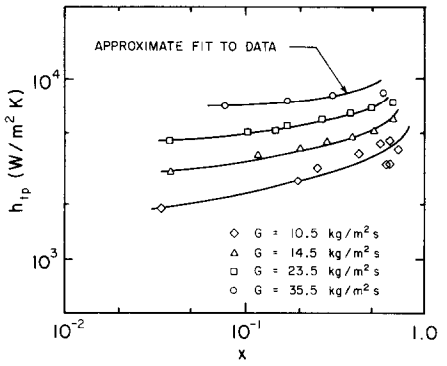

FIG. 11. Measured local heat transfer coefficients for convective boiling of *n*-butanol in a vertical channel with offset strip fins.

water, methanol and *n*-butanol, respectively. The variation of h_{tp} with x is shown for low to moderate values of G in these plots. Additional data were obtained for higher values of G, but the systematic variation of h_{tp} with x was not determined. The measured value of h_{tp} is seen to increase with increasing G and x for all three fluids. The data obtained at higher mass flow levels were consistent with the trends observed in Figs. 9–11. The variations of h_{tp} with x and G shown in these figures are qualitatively similar to those obtained by Robertson [5] and Robertson and Lovegrove [8] for a fully heated channel with offset strip fins.

It can also be seen in Figs. 9 and 10 that for the same G and x values, the h_{tp} value for water is much higher than the value of h_{tp} for methanol. The corresponding h_{tp} value for *n*-butanol was also much lower than the water value. The lower h_{tp} values for the alcohols appear to be a consequence of the lower molecular conductivities of these liquids relative to that of water.

ANALYSIS

The data described in the previous section indicate that the local heat transfer coefficient for annular film flow boiling in offset fin geometries is a function of the mass flux, quality and the properties of the liquid and vapor. In this section, an approximate model of the liquid film flow is used to derive a correlation for the heat transfer coefficient which accounts for these variables.

The film-flow model proposed here is similar to models proposed in other studies of annular flow in offset fin geometries [6, 7, 9] and round tubes [12]. However, this model differs in that several assumptions are incorporated which are based on the observed behavior of the two-phase flow during our experiments. The flow of liquid in the film is assumed to be weakly turbulent, which is consistent with the range of film Reynolds numbers encountered for the conditions tested here. Although intermittent waves on the surface of the liquid film were sometimes observed in our experiments, in the approximate analytical model developed here, the effects of waves are neglected and the interface is assumed to be smooth. It is further assumed that the amount of liquid entrained in the vapor flow is small and that virtually all the liquid flows in the film on the walls. This is consistent with our visual observations which indicated that little entrained liquid was present during most of the boiling process. Recall that small amounts of liquid were observed being shed from the downstream edge of the fin only for brief intermittent intervals.

As in many of the previous analyses of liquid film flow, it is assumed here that the film is thin and that downstream convection is negligible compared with transport of energy and momentum across the film. It is further assumed that the downward gravity force and the upward effect of the pressure gradient within the liquid film act to cancel each other so that the shear stress is virtually constant across the film. Calculations using pressure drop correlations for round tubes indicate that this approximation is justifiable for the conditions considered here. A similar assumption was also employed by Robertson [6] in his film-flow analysis of convective boiling in a fully-heated channel with offset strip fins.

With the assumptions noted above, the relations for the mass, momentum and energy balances in the liquid film on the channel walls can be written

$$\frac{G(1-x)A_o}{P_W\mu_f} = \int_0^{\delta^+} u^+ \, dy^+ \tag{3}$$

$$1 = \left(1+\frac{\varepsilon_M}{\nu_f}\right)\frac{du^+}{dy^+} \tag{4}$$

$$\left(\frac{T_W - T_{SAT}}{q''}\right)\frac{k_f\sqrt{\tau_o/\rho_f}}{\nu_f} = \int_0^{\delta^+} dy^+ \Big/ \left(1+\frac{Pr_f}{Pr_t}\frac{\varepsilon_M}{\nu_f}\right) \tag{5}$$

where u^+ and y^+ are the usual non-dimensional variables for turbulent flow near a wall. Note also that the wall temperature even on the fins is assumed to equal T_W, the temperature of the prime surface of the channel. This is done because the value of hA_F obtained from this analysis will be corrected by multiplying by the fin efficiency to obtain the contributions of the fins to the total heat transfer.

The liquid film is assumed to be weakly turbulent such that

$$\frac{\varepsilon_M}{\nu_f} > 0, \quad \text{but} \quad \frac{\varepsilon_M}{\nu_f} \ll 1. \tag{6}$$

Hence, the transport of momentum in the film is, to a first approximation, assumed to be a laminar process. Equation (4) can then be integrated to obtain $u^+ = y^+$ and this result can be inserted into (3) to obtain

$$\delta^+ = \sqrt{Re_f/2}. \tag{7}$$

It is further assumed here that the Prandtl number is sufficiently large that, even though ε_M/ν_f is small,

$Pr_f\varepsilon_M/\nu_f$ is not small. The $Pr_f\varepsilon_M/\nu_f Pr_t$ term in equation (5) must therefore be retained. Hence, at the moderate to large values of Prandtl number considered here, the weak turbulence in the film will affect the transport of heat, even though it has little effect on momentum transport.

To evaluate ε_M/ν_f in the region near the channel wall, the well-known Von Karman mixing length model is used. Taking the mixing length equal to κy and using the fact that $u^+ = y^+$ in the film, it is easily shown that

$$\frac{\varepsilon_M}{\nu_f Pr_t} = \frac{\kappa^2}{Pr_t}(y^+)^2. \tag{8}$$

As discussed by Hinze [13], ε_M/ν has usually been assumed to be proportional to $(y^+)^3$ or $(y^+)^4$ very near the surface in a wall turbulent shear flow. However, the data of Hughmark [14] suggest that

$$\frac{\varepsilon_M}{\nu_f Pr_t} \propto (y^+)^{1.9} \quad \text{for} \quad 12 < y^+ < 35. \tag{9}$$

Hence, equation (8) is consistent with data at the outer edge of the conduction sublayer where the eddy diffusivity of heat is expected to be most important in the films considered here.

In addition, previous studies [15, 16] indicate that the turbulent diffusivity of heat should also approach zero proportional to $(\delta^+ - y^+)^2$ to account for the damping of turbulence near the liquid–vapor interface. To maintain consistency with these conclusions and equation (8), the distribution of the diffusivity across the film was assumed to be

$$\frac{\varepsilon_M}{\nu_f Pr_t} = \begin{cases} \kappa^2(y^+)^2/Pr_t & \text{for} \quad 0 \leqslant y^+ \leqslant \delta^+/2 \\ \kappa^2(\delta^+ - y^+)^2/Pr_t & \text{for} \quad \delta^+/2 < y^+ \leqslant \delta^+. \end{cases} \tag{10}$$

As noted above, the objective of the present analysis was to derive a closed-form relation for the heat transfer coefficient. The relations given by (10) were therefore chosen to approximate the variation of the turbulent diffusivity across the film because they are consistent with the physical arguments described above, and yet are simple enough to permit us to obtain an explicit relation for h_{tp}.

Since τ_o must be related to the frictional component of the two-phase pressure drop in the channel formed by two adjacent fins, the following relation can be written for $\sqrt{\tau_o/\rho_f}$:

$$\sqrt{\tau_o/\rho_f} = (\nu_f/d_h)\phi_f\, Re_f\sqrt{f_f/2} \tag{11}$$

where f_f is the friction factor for the liquid flowing alone in the channel formed by two adjacent fins. Note that this is not the same as the friction factor for the entire matrix, which includes the effects of form drag on the fins. Since f_f applies only to the channel between fins, the modified Reynolds analogy is used to relate it to the Colburn j-factor, $StPr^{2/3}$.

$$f_f/2 = St_f Pr_f^{2/3}. \tag{12}$$

Here, it is assumed that the Colburn j-factor for the partially heated channel, $St_{fp}Pr_f^{2/3}$, is given by

$$St_{fp}Pr_f^{2/3} = A\, Re_{fp}^{-n}, \quad Re_{fp} = G(1-x)d_{hp}/\mu_f \tag{13}$$

and that the Colburn j-factor for an identical, fully heated channel is given by the same relation with d_{hp} replaced by d_h

$$St_f Pr_f^{2/3} = A\, Re_f^{-n}, \quad Re_f = G(1-x)d_h/\mu_f. \tag{14}$$

Integrating the RHS of equation (5) using the relations in (10), and substituting (7) and (11)–(14), the following relation is obtained for h_{tp}

$$h_{tp} = \frac{q''}{T_W - T_{SAT}} = \left(\frac{k_f}{d_{hp}}\right)\left(\frac{\kappa\phi_f}{2I}\right)\sqrt{\frac{A\,Pr_f}{Pr_t}}\, Re_{fp}^{1-n/2}\left(\frac{d_{hp}}{d_h}\right)^{n/2} \tag{15}$$

where

$$I = \tan^{-1}[\kappa\sqrt{Pr_f Re_{fp}/8Pr_t}\,\sqrt{d_h/d_{hp}}]. \tag{16}$$

Non-dimensionalizing by dividing through by h_{fp}, and using (13) together with the definition of St_{fp}, we obtain

$$\left(\frac{h_{tp}}{h_{fp}}\right)\frac{2I\sqrt{A\,Pr_t}}{\kappa\, Re_{fp}^{n/2}\, Pr_f^{1/6}}\left(\frac{d_h}{d_{hp}}\right)^{n/2} = \phi_f. \tag{17}$$

Recommended values of the Von Karman constant, $\kappa = 0.40$, and turbulent Prandtl number, $Pr_t = 0.90$ [13, 15] are substituted into (17) together with (16) to obtain:

$$\left(\frac{h_{tp}}{h_{fp}}\right)\frac{4.74\sqrt{A}\,\tan^{-1}[0.149\sqrt{Re_{fp}Pr_f}\,\sqrt{d_h/d_{hp}}]}{Re_{fp}^{n/2}\, Pr_f^{1/6}(d_{hp}/d_h)^{n/2}} = \phi_f. \tag{18}$$

At the present time, there are no correlations available to predict ϕ_f for turbulent–turbulent, two-phase flow in offset fin geometries. Hence, as a first approximation, the turbulent–turbulent correlation of Lockhart and Martinelli [17] is used for ϕ_f:

$$\phi_f = \left[1 + \frac{20}{X_{tt}} + \frac{1}{X_{tt}^2}\right]^{1/2} \tag{19}$$

where X_{tt} is defined as

$$X_{tt} = [(dp/dz)_{Ff}/(dp/dz)_{Fg}]^{1/2}. \tag{20}$$

Consistent with the Reynolds analogy, (12), and equation (14), it is assumed that

$$f_f = 2A\, Re_f^{-n} \tag{21}$$

and

$$f_g = 2A\, Re_g^{-n}, \quad Re_g = Gxd_h/\mu_g. \tag{22}$$

Using (21) and (22) with (20), it is easily shown that X_{tt} is given by

$$\frac{1}{X_{tt}} = \left(\frac{\rho_f}{\rho_g}\right)^{1/2}\left(\frac{\mu_g}{\mu_f}\right)^{n/2}\left(\frac{x}{1-x}\right)^{1-n/2}. \tag{23}$$

Thus, with the definition of X_{tt} given by (23), (18) and

(19) form a complete correlation for the convective boiling heat transfer coefficient:

$$\Psi = \left(\frac{h_{tp}}{h_{fp}}\right)\frac{4.74\sqrt{A}\tan^{-1}\left[0.149\sqrt{Re_{fp}Pr_f}\sqrt{d_h/d_{hp}}\right]}{Re_{fp}^{n/2}\,Pr_f^{1/6}(d_{hp}/d_h)^{n/2}} = \left[1+\frac{20}{X_{tt}}+\frac{1}{X_{tt}^2}\right]^{1/2}. \quad (24)$$

It is interesting to note that the $\tan^{-1}$ term approaches a constant at large values of $Re_{fp}Pr_f$ and also that $n/2$ is usually small, so the dependence of Ψ on Re_{fp} is weak. If we neglect the Re_{fp} dependence and assume the $\tan^{-1}$ term is constant, (24) implies that

$$\frac{h_{tp}}{h_{fp}}Pr_f^{-1/6} = f(1/X_{tt}). \quad (25)$$

The relation (25) above is very similar to the correlation recently proposed by Bennett and Chen [18] for the macroscopic (non-nucleate boiling) contribution to the convective boiling heat transfer coefficient for vertical round tubes. Their correlation is of the form

$$\frac{h_{tp}}{h_f}Pr_f^{-0.296} = f(1/X_{tt}). \quad (26)$$

Hence, although the correlating parameter used in (24) has slightly different dependence on Reynolds and Prandtl number, it is similar in the form to that used in the Bennett and Chen [18] correlation for round tubes.

The measured heat transfer data obtained here for water, methanol and *n*-butanol are plotted in terms of Ψ and $1/X_{tt}$ in Figs. 12–14. In these figures the open symbols correspond to annular flow and the solid symbols indicate churn flow. In calculating Ψ, the values of n and A were taken from the turbulent correlation in Fig. 3 to be 0.36 and 0.215, respectively. Also shown in Figs. 12–14 is the curve corresponding to equation (24).

In Figs. 12–14, it can be seen that the data in the annular flow regime agree very well with the model prediction for all three fluids tested here. The agreement is, in fact, surprisingly good considering that the analysis

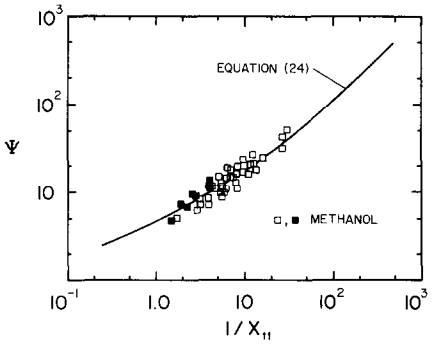

FIG. 13. Comparison of the measured heat transfer data for methanol with the correlation (24) developed from the analytical model. The solid symbols designate churn flow and the open symbols designate annular film flow.

assumes a moderate to large liquid Prandtl number, and the liquid Prandtl numbers for these fluids are all less than 8.7. Even for data in the churn flow regime, agreement with the correlation is quite good, although the scatter about the curve is a bit larger, particularly for water and *n*-butanol. The increased scatter about the model prediction in the churn flow regime is somewhat expected, since the model does not account for the weakly oscillatory behavior of the flow which has been observed for these conditions.

CONCLUSIONS

Measured local heat transfer coefficients have been obtained for convective boiling in a vertical channel with offset fins which was heated on one side only. Heat transfer data have been reported for convective boiling of water, methanol and *n*-butanol over wide ranges of mass flux and quality. In addition, the two-phase flow in the channel was visually observed and photographed during the convective boiling process to determine the flow regime at the locations where heat transfer data were obtained.

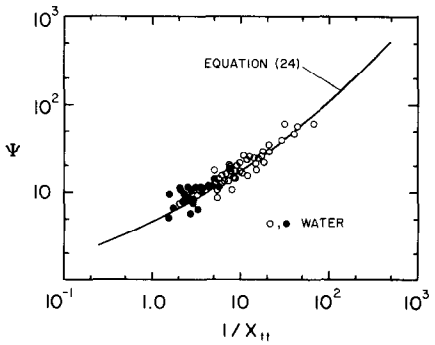

FIG. 12. Comparison of the measured heat transfer data for water with the correlation (24) developed from the analytical model. The solid symbols designate churn flow and the open symbols designate annular film flow.

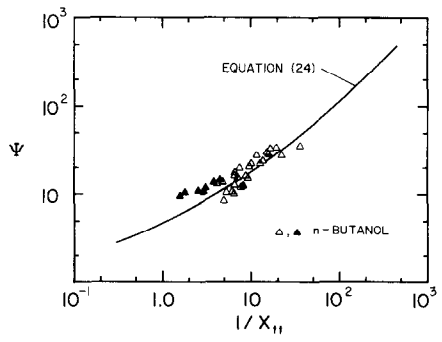

FIG. 14. Comparison of the measured heat transfer data for *n*-butanol with the correlation (24) developed from the analytical model. The solid symbols designate churn flow and the open symbols designate annular film flow.

Visual observations indicated that for the relatively low pressure conditions considered here, the two-phase flow takes on an annular configuration a short distance downstream of the beginning of saturated boiling. Beyond that point, the flows studied here were in either the churn-flow or annular flow regime. In these regimes, nucleate boiling was suppressed over virtually the entire heated surface. For all three liquids tested here, the measured value of the local convective boiling heat transfer coefficient was found to increase with increasing quality or mass flux.

These observed flow characteristics and trends in the heat transfer data are qualitatively similar to those expected to occur in a plain, round tube under comparable conditions. However, in some ways, the convective boiling process in the partially heated channel with offset strip fins was found to be distinctly different from comparable boiling circumstances in round tubes. For the offset fin geometry tested here, the transition from churn flow to annular flow was found to occur at a lower value of $\rho_g j_g^2$ than the values suggested by Hewitt and Roberts [10] or Wallis [11] for vertical round tubes. In terms of the j_g^* parameter defined by Wallis [11], the transition in the geometry considered here occurred approximately at $j_g^* = 0.5$. Wallis [11] suggested a slightly higher value, $j_g^* = 0.9$, for round tubes.

For annular flow convective boiling in a uniformly-heated, vertical, round tube, the film is relatively uniform around the tube perimeter, and complete dryout of the liquid film usually occurs over a very short distance downstream of the first appearance of dry areas on the tube wall. For the partially heated channel with offset strip fins, the thickness of the liquid film varies over the heated surface, and consequently, the dryout characteristics are quite different. In our experiments, it was observed that localized dry patches on the heated surface may occur at qualities as low as 0.4. The size of these patches increased with downstream distance until the entire surface was dry. As a result, the heated surface may be partially dry over a significant portion of the channel length.

It was also observed that the offset fins act to transfer liquid from the adiabatic wall of the partially heated channel to the fins themselves and to the heated wall. This transfer acts to delay complete dryout of the heated surface, and thereby avoids overheating of the channel wall. In a partially heated tube without offset fins, no such transfer of liquid would occur. This feature of convective boiling in offset fin geometries may be particularly attractive in applications where dryout of the heated wall of a partially-heated coolant passage would adversely affect performance.

An approximate model of the transport in the liquid film during the boiling process has also been presented. Although a number of simplifying assumptions have been incorporated into this model, the predictions of the convective boiling correlation derived from the model agree well with our annular flow and churn-flow data for all three fluids tested here. The form of this correlation, given by equation (24), may be a useful starting point for development of a general correlation technique for predicting the convective boiling heat transfer performance of vertical channels with offset strip fins. However, more data for other geometries is needed to fully assess the usefulness of such a correlation.

Acknowledgements—The authors wish to acknowledge support for this research by the National Science Foundation under research grant No. CBT-8451781. The assistance of Susan Bavonese in preparation of the manuscript is also appreciated.

REFERENCES

1. H. Panitsidis, R. D. Gresham and J. W. Westwater, Boiling of liquids in a compact plate-fin heat exchanger, *Int. J. Heat Mass Transfer* **18,** 37–42 (1975).
2. C. C. Chen, J. V. Loh and J. W. Westwater, Prediction of boiling heat transfer duty in a compact plate-fin heat exchanger using the improved local assumption, *Int. J. Heat Mass Transfer* **24,** 1907–1912 (1981).
3. C. C. Chen and J. W. Westwater, Application of the local assumption for the design of compact heat exchangers for boiling heat transfer, *Trans. Am. Soc. mech. Engrs*, Series C, *J. Heat Transfer* **106,** 204–209 (1984).
4. V. B. Galezha, I. P. Usyukin and K. D. Kan, Boiling heat transfer with freons in finned-plate heat exchangers, *Heat Transfer–Sov. Res.* **8,** 103–110 (1976).
5. J. M. Robertson, Boiling heat transfer with liquid nitrogen in brazed-aluminum plate-fin heat exchangers, *A.I.Ch.E. Symp. Ser.* **75,** 151–164 (1979).
6. J. M. Robertson, The correlation of boiling coefficients in plate-fin heat exchanger passages with a film-flow model, *Proc. 7th Int. Heat Transfer Conference*, Munich, Vol. 6, pp. 341–345 (1982).
7. J. M. Robertson, The prediction of convective boiling coefficients in serrated plate-fin passages using an interrupted liquid-film flow model. In *Basic Aspects of Two-Phase Flow and Heat Transfer*, HTD-Vol. 34, pp. 163–171. ASME, New York (1984).
8. J. M. Robertson and P. C. Lovegrove, Boiling heat transfer with freon 11 (R11) in brazed aluminum plate-fin heat exchangers, *Trans. Am. Soc. mech. Engrs*, Series C, *J. Heat Transfer* **105,** 605–610 (1983).
9. D. Yung, J. J. Lorenz and C. Panchal, Convective vaporization and condensation in serrated-fin channels. In *Heat Transfer in Ocean Thermal Energy Conversion Systems*, HTD-Vol. 12, pp. 29–37. ASME, New York (1980).
10. G. F. Hewitt and D. N. Roberts, Studies of two-phase flow patterns by simultaneous X-ray and flash photography, AERE Report AERE-M 2159, HMSO (1969).
11. G. B. Wallis, *One Dimensional Two-Phase Flow*, Chap. 11. McGraw-Hill, New York (1969).
12. H. R. Kunz and S. Yerazunis, An analysis of film condensation, film evaporation and single phase heat transfer for liquid Prandtl numbers from 10^{-3} to 10^4, *Trans. Am. Soc. mech. Engrs*, Series C, *J. Heat Transfer* **91,** 413–420 (1969).
13. J. O. Hinze, *Turbulence*, 2nd Edn, Chap. 7. McGraw-Hill, New York (1975).
14. G. A. Hughmark, Heat and mass transfer for turbulent pipe flow, *A.I.Ch.E. Jl* **17,** 902–909 (1971).
15. O. C. Sandall, O. T. Hanna and C. L. Wilson, III, Heat transfer across turbulent falling liquid films, *A.I.Ch.E. Symp. Ser.* **80,** 3–9 (1984).

16. A. F. Mills and D. K. Chung, Heat transfer across turbulent falling films, *Int. J. Heat Mass Transfer* **16**, 693–701 (1973).
17. R. W. Lockhart and R. C. Martinelli, Proposed correlation of data for isothermal two-phase, two-component flow in pipes, *Chem. Engng Prog.* **45**, 39–48 (1949).
18. D. L. Bennett and J. C. Chen, Forced convective boiling in vertical tubes for saturated pure components and binary mixtures, *A.I.Ch.E. Jl* **26**, 454–461 (1980).

EBULLITION EN FILM ANNULAIRE D'UN LIQUIDE EN ECOULEMENT DANS UN CANAL VERTICAL PARTIELLEMENT CHAUFFE ET MUNI D'AILETTES

Résumé—Des visualisations d'écoulement et des données locales de transfert thermique sont présentées pour l'ébullition en film annulaire de liquides saturés dans un canal vertical muni d'ailettes. Une section d'essai spécial permet une observation directe du mécanisme d'ébullition pendant le mesure des coefficients locaux de transfert thermique en plusieurs points le long du canal. Une paroi du canal est chauffée tandis que les parois opposée et latérale sont adiabatiques. Les coefficients de transfert sur la portion chauffée du canal sont obtenus pour l'ébullition de l'eau, du méthanol et du *n*-butanol à la pression atmosphérique, dans de larges domaines de débit et de qualité. Les photographies montrent l'absence d'ébullition nucléée quand l'écoulement est dans le régime d'écoulement avec film. Pour la matrice d'ailettes étudiée ici, on n'observe pas d'assèchement complet du film sur la surface chaude en une seule région en aval. On observe des taches sèches qui se forment à des points spécifiques de la matrice, et le réseau croît en taille avec la distance en aval jusqu'à ce que le film entier ait disparu. Un modèle analytique approché du transport dans le film liquide est présenté. Une formule pour le coefficient de transfert est obtenu par ce modèle et elle s'accorde bien avec les données.

STRÖMUNGSSIEDEN BEI RINGSTRÖMUNG IN EINEM TEILWEISE BEHEIZTEN SENKRECHTEN KANAL MIT STREIFENFÖRMIGEN VERSETZTEN RIPPEN

Zusammenfassung—Es werden Photographien der Strömung und örtliche Wärmeübergangskoeffizienten für das Strömungssieden gesättigter Flüssigkeiten bei Ringströmung in einem senkrechten Kanal mit versetzten streifenförmigen Rippen dargestellt. Es wurde eine spezielle Meßstrecke verwendet, welche direkte visuelle Beobachtungen des Siedevorganges und gleichzeitige Messung des örtlichen Wärmeübergangskoeffizienten an verschiedenen Punkten entlang des Kanals erlaubte. Eine Kanalwand wurde beheizt, während die beiden benachbarten und die gegenüberliegende Wand adiabat waren. Örtliche Wärmeübergangskoeffizienten am beheizten Teil der Kanalwand wurden für konvektives Sieden von Wasser, Methanol und *n*-Butanol bei Atmosphärendruck über einen weiten Bereich der Massenstromdichte und des Dampfgehaltes bestimmt. Photographien der Strömung zeigen, daß tatsächlich kein Blasensieden vorhanden ist, wenn Filmströmung vorliegt. Für die hier untersuchte Rippenanordnung wurde ein vollständiges Austrocknen des Films an einer einzelnen Stelle strömungsabwärts an der beheizten Oberfläche nicht beobachtet. Stattdessen wurden trockene Flächen festgestellt, die sich an spezifischen Stellen bilden. Diese Flächen wachsen in ihrer Größe strömungsabwärts an, bis der Film vollständig verschwunden ist. Ein analytisches Näherungsmodell für den Transport im flüssigen Film wird ebenfalls dargestellt. Es wird eine Korrelation in geschlossener Form für den Wärmeübergangskoeffizienten beim Sieden aus diesem Modell abgeleitet. Es zeigt sich eine gute Übereinstimmung mit den gemessenen Werten

КИПЕНИЕ ПРИ ПЛЕНОЧНОМ ТЕЧЕНИИ ЖИДКОСТЕЙ В ЧАСТИЧНО ОБОГРЕВАЕМОМ КОЛЬЦЕВОМ ВЕРТИКАЛЬНОМ КАНАЛЕ С ПЛАСТИНЧАТЫМ ОРЕБРЕНИЕМ

Аннотация—Представлены фотографии по визуализации течения и данные по измерениям локального теплопереноса при пленочном течении жидкостей в кольцевом вертикальном канале с пластинчатым оребрением. Использовалась специальная опытная установка, дающая возможность прямой визуализации процесса кипения при одновременном измерении коэффициентов локального теплопереноса в нескольких точках вдоль канала. Одна стенка канала нагревалась, в то время как противоположная и боковые были адиабатическими. Коэффициенты локального теплопереноса на нагреваемых участках стенки измерены для кипящих воды, метанола и *n*-бутанола при атмосферном давлении в широком диапазоне потоков массы и характера поверхности. Фотографии течения свидетельствуют о том, что при пленочном течении жидкости пузырькового кипения практически не существует. Для исследуемой системы ребер не наблюдалось полного высыхания пленки на нагреваемой поверхности, оно имело место лишь в отдельных точках по течению. Замечено, что сухие участки образуют на матрице характерные зоны, причем размеры участков растут по потоку. Представлена приближенная аналитическая модель переноса в пленке жидкости. Из модели выведено уравнение замкнутого типа для коэффициента теплообмена при кипении, которое хорошо согласуется с данными измерений.